

RESEARCH ARTICLE

# Preclinical Evaluation of Radiolabeled DOTA-Derivatized Cyclic Minigastrin Analogs for Targeting Cholecystokinin Receptor Expressing Malignancies

Elisabeth von Guggenberg,<sup>1</sup> Christine Rangger,<sup>1</sup> Jane Sosabowski,<sup>2</sup> Peter Laverman,<sup>3</sup> Jean-Claude Reubi,<sup>4</sup> Irene Johanna Virgolini,<sup>1</sup> Clemens Decristoforo<sup>1</sup>

<sup>1</sup>Department of Nuclear Medicine, Innsbruck Medical University, Anichstrasse 35, 6020 Innsbruck, Austria

<sup>2</sup>Centre for Molecular Oncology and Imaging, Barts and the London, Queen Mary's School of Medicine and Dentistry, London, UK

<sup>3</sup>Department of Nuclear Medicine, Radboud University Nijmegen Medical Centre, Nijmegen, The Netherlands

<sup>4</sup>Department of Pathology, University of Berne, Berne, Switzerland

## Abstract

**Purpose:** Targeting of cholecystokinin receptor expressing malignancies such as medullary thyroid carcinoma is currently limited by low *in vivo* stability of radioligands. To increase the stability, we have developed and preclinically evaluated two cyclic 1,4,7,10-tetraazacyclododecane-1,4,7,10-tetraacetic acid (DOTA)-minigastrin analogs radiolabeled with <sup>111</sup>In and <sup>68</sup>Ga.

**Procedures:** Radiolabeling efficiency, *in vitro* characterization, cholecystokinin receptor subtype 2 (CCK-2) binding in human tumor tissues, and cell internalization on CCK-2 receptor expressing AR42J cells, as well as biodistribution and small animal imaging in two different mouse xenograft models were studied.

**Results:** High receptor affinity and receptor-mediated uptake of the radioligands in AR42J cells was confirmed *in vitro*. <sup>111</sup>In-labeled cyclic DOTA-peptides showed a specific tumor uptake of ~1% ID/g *in vivo*, <sup>68</sup>Ga-labeled analogs of ~3% ID/g. Small animal SPECT imaging resulted to be superior with <sup>111</sup>In-DOTA-cyclo-MG2 in comparison with <sup>111</sup>In-DOTA-cyclo-MG1.

**Conclusions:** Cyclic DOTA-minigastrin analogs are promising candidates for gastrin receptor scintigraphy and targeted radionuclide therapy.

**Key words:** Cholecystokinin receptors, Medullary thyroid carcinoma, Neuroendocrine tumors, Peptides, Radionuclides, Receptor targeting, Molecular imaging, Targeted therapy

## Introduction

Targeting receptors on human tumors has been very successful using radiolabeled somatostatin (SS) analogs, but is limited to specific neoplasms overexpressing mainly the SS receptor subtype 2 [1]. Somatostatin receptor scintigraphy (SRS) is considered an established procedure

for the diagnosis and staging of gastro-entero-pancreatic tumors and their metastases, and patients treated with <sup>90</sup>Y- and <sup>177</sup>Lu-labeled SS analogs show a reduction in tumor size as well as improved quality of life and overall prognosis [2]. The cholecystokinin receptor subtype 2 (CCK-2) has also been shown to be over-expressed in numerous neuroendocrine tumors, in particular medullary thyroid carcinoma (MTC), neuroendocrine gut tumors, and stromal tumors [3].

Various gastrin and CCK analogs with high affinity to the CCK-2 receptor have been developed to deliver peptide

Correspondence to: Elisabeth von Guggenberg; e-mail: elisabeth.vonguggenberg@uki.at

receptor-targeted imaging and therapy with radionuclides to these tumor types. In particular, MTC is a major target of interest, as conventional imaging with radiolabeled SS analogs often is not successful [4]. Gastrin receptor scintigraphy (GRS) and targeted radionuclide therapy (TRT) of MTC was first reported in humans using D-Glu<sup>1</sup>-minigastrin (MG0) based on native minigastrin (LEEEEEAYGWMDF-NH<sub>2</sub>, MG), derivatized with diethylenetriaminepentaacetic acid for radiolabeling with <sup>111</sup>In and <sup>90</sup>Y [5]. GRS has shown a higher tumor detection rate as compared to both SRS and 2-deoxy-2-[<sup>18</sup>F]fluoro-D-glucose positron emission tomography (PET) in MTC [6] and can provide additional information in the detection of neuroendocrine tumors, especially if SRS is negative. GRS seems to be promising also for the detection of small-cell lung cancer [7] and shows potential also for the diagnosis and treatment of colorectal and pancreatic cancer [8]. Radioligands based on MG0 display a very high kidney uptake *in vivo* [9–11] limiting the application in humans [4]. The mechanism of kidney uptake has been studied extensively and is related to the penta-Glu motif in the peptide sequence [12, 13]. A MG analog without the penta-Glu motif in position 2–6 (MG11), was developed and radiolabeled with different radionuclides [14–17]. Besides clearly reduced kidney uptake and retained tumor uptake, these radioligands displayed reduced stability *in vitro* and rapid enzymatic degradation *in vivo*, possibly leading to impaired imaging characteristics in first clinical trials [18]. A progressive decrease in enzymatic stability of the peptide conjugate with decreasing number of glutamic acid residues was confirmed [19].

Under the premise that the radioligands developed so far are not suitable for clinical application, we have investigated new stabilization strategies. Since linear CCK8 and gastrin analogs exist in various folded conformations in solution [20], we have designed a cyclic MG analog based on MG11, containing unnatural amino acids in the peptide chain and a cyclic constraint introduced through an internal amide bond, cyclo[ $\gamma$ -D-Glu-Ala-Tyr-D-Lys]-Trp-Met-Asp-Phe-NH<sub>2</sub> (cyclo-MG1). Met in position 6 was additionally replaced with Nle to produce cyclo[ $\gamma$ -D-Glu-Ala-Tyr-D-Lys]-Trp-Nle-Asp-Phe-NH<sub>2</sub> (cyclo-MG2). For comparative studies, the linear peptide analog,  $\gamma$ -D-Glu-Ala-Tyr-D-Lys-Trp-Met-Asp-Phe-NH<sub>2</sub> (linear-MG1) was also synthesized. In a previous study, we have derivatized these peptide analogs with hydrazino nicotinamide (HYNIC) for the labeling with <sup>99m</sup>Tc [21]. In the present study, we have derivatized the peptide analogs with 1,4,7,10-tetraazacyclododecane-1,4,7,10-tetraacetic acid (DOTA) to enable labeling with trivalent radioisotopes, such as <sup>111</sup>In for single-photon emission computed tomography (SPECT), <sup>68</sup>Ga for PET, and especially also <sup>90</sup>Y and <sup>177</sup>Lu for therapeutic applications. The preclinical evaluation including radiolabeling with <sup>111</sup>In and <sup>68</sup>Ga, characterization of stability and receptor binding *in vitro*, as well as biodistribution studies and evaluation of the imaging characteristics in two different mouse xenograft models revealed some

differences between the peptide analogs radiolabeled with different radioisotopes. Interestingly, <sup>68</sup>Ga-labeled cyclic DOTA-peptides showed a tumor uptake which was comparable to that of <sup>99m</sup>Tc-labeled cyclic HYNIC-peptides, whereas for <sup>111</sup>In-labeled cyclic DOTA-peptides, a much lower tumor uptake was observed.

## Materials and Methods

### Materials

All chemicals obtained commercially were analytical grade and used without further purification unless otherwise stated.

<sup>111</sup>InCl<sub>3</sub> was purchased from Perkin Elmer (Shelton, CT, USA). <sup>68</sup>GaCl<sub>3</sub> was obtained from a commercial <sup>68</sup>Ge/<sup>68</sup>Ga-generator (Cyclotron Co Ltd, Obninsk, Russia) with nominal activity of 925 MBq and eluted with biochemical grade 0.1 M HCl (Sigma-Aldrich, Steinheim, Germany).

The two cyclic MG analogs, DOTA-cyclo[ $\gamma$ -D-Glu-Ala-Tyr-D-Lys]-Trp-Met-Asp-Phe-NH<sub>2</sub> (DOTA-cyclo-MG1) and DOTA-cyclo[ $\gamma$ -D-Glu-Ala-Tyr-D-Lys]-Trp-Nle-Asp-Phe-NH<sub>2</sub> (DOTA-cyclo-MG2), and the linear MG analog, DOTA- $\gamma$ -D-Glu-Ala-Tyr-D-Lys-Trp-Met-Asp-Phe-NH<sub>2</sub> (DOTA-linear-MG1), were synthesized by piChem (Graz, Austria). The peptide analogs were characterized using MALDI-TOF mass spectrometry and analyzed by reversed phase high-performance liquid chromatography (RP-HPLC) using a gradient system of water containing 0.1% trifluoroacetic acid (TFA) and acetonitrile (ACN) containing 0.1% TFA to confirm a purity >95%. The structure for DOTA-cyclo-MG1 and DOTA-cyclo-MG2 is shown in Fig. 1.

### Labeling with Indium-111 and Gallium-68

For labeling with <sup>111</sup>In, the DOTA-peptides (40  $\mu$ g) were incubated with 50  $\mu$ L <sup>111</sup>InCl<sub>3</sub> solution (74–111 MBq in 0.05 M HCl) and 100  $\mu$ L of a solution containing sodium acetate trihydrate (55.4 mg/mL in water) and gentisic acid (37 mg/mL in water) adjusted to pH 5.0 with 0.05 N HCl, in a total volume of ~0.2 mL. The optimal reaction

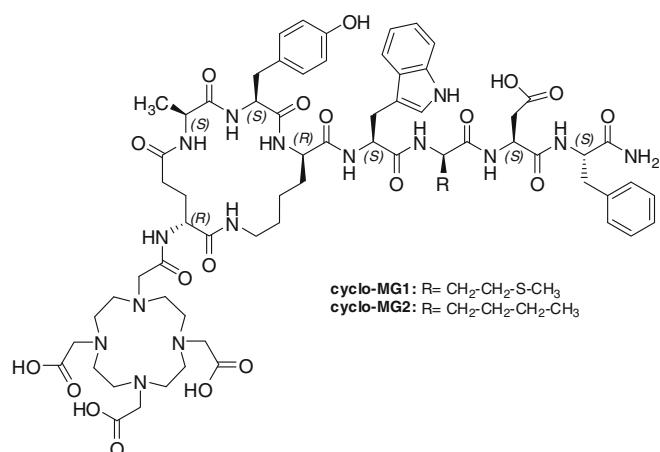


Fig. 1. Structure of DOTA-cyclo-MG1 and DOTA-cyclo-MG2.

conditions in terms of reaction temperature and incubation time to obtain radiochemical yields >95% were evaluated.

For labeling with  $^{68}\text{Ga}$ , the DOTA-peptides (20  $\mu\text{g}$ ) were incubated with a 0.5 mL fraction of the generator eluate (containing 148–185 MBq  $^{68}\text{GaCl}_3$ ) and 50  $\mu\text{L}$  sodium acetate solution (160 mg/mL in water) in a total volume of  $\sim 0.6$  mL. Again the optimal reaction conditions to achieve high radiochemical yields were evaluated.

Radiochemical analysis of the radiolabeled peptide conjugates was performed by RP-HPLC on a Dionex P680 chromatography system (Vienna, Austria) with UV detection at 220 nm (Spectra Chrom 100 variable UV detector, Spectra Physics, Darmstadt, Germany) and radiometric detection (Raytest, Straubenhardt, Germany). Data were processed using Dionex Chromeleon software. The system was equipped with an ACE3 C18 column  $150 \times 3$  mm (Advanced Chromatography Technology, Aberdeen, UK) and eluted using a gradient system of water containing 0.1% TFA (solvent A) and ACN containing 0.1% TFA (solvent B) at a flow rate of 0.6 mL/min: 0–9 min linear gradient from 10% to 60% B, 9–12 min 60% B.

### Characterization of the Radiolabeled Peptides *In Vitro*

*In vitro* characterization was performed only for the cyclic DOTA-peptides radiolabeled with  $^{111}\text{In}$ . Due to the short half-life of  $^{68}\text{Ga}$ , these studies were not performed with the  $^{68}\text{Ga}$ -labeled cyclic DOTA-peptides.

The stability of the radiolabeled peptides was investigated by incubation at a concentration of 500–1,000 pmol peptide/mL at  $37^\circ\text{C}$  for up to 24 h in phosphate-buffered saline (PBS) and fresh human plasma. Degradation of the radioligands was assessed by radio-HPLC; plasma samples were precipitated with ACN and centrifuged at  $2,000 \times g$  for 2 min (centrifuge 5424, Eppendorf, Hamburg, Germany).

For the determination of octanol/water partition coefficients, the radiolabeled peptides in 500  $\mu\text{L}$  PBS (pH 7.4) were added to 500  $\mu\text{L}$  octanol in an Eppendorf microcentrifuge tube in six replicates. The mixture was vigorously vortexed over a period of 15 min at room temperature (RT). After centrifugation at  $9,000 \times g$  for 2 min the radioactivity of 50  $\mu\text{L}$  aliquots of both layers was measured in a gamma counter (Compugamma 1282, LKB/Wallac, Turku, Finland) and the log  $P$  value was calculated.

For protein binding assessment the radioligands were incubated in duplicates at a concentration of 500–1,000 pmol/mL in fresh human plasma at  $37^\circ\text{C}$  and analyzed for up to 4 h by Sephadex G-50 size-exclusion chromatography (MicroSpin, GE-Healthcare Life Sciences, Vienna, Austria). Protein binding was determined by measuring the activity on the column and in the eluate in a gamma counter.

The stability of the radiolabeled peptides to enzymatic degradation was assessed by incubation in liver and kidney homogenates. Liver or kidneys freshly excised from rat were rapidly rinsed and homogenized in 20 mM HEPES buffer pH 7.3 with an Ultra-Turrax T8 homogenizer (IKA-Werke, Staufen, Germany) for 1 min at RT. The radiolabeled peptides were incubated with fresh 30% homogenates at a concentration of 500–1,000 pmol peptide/mL at  $37^\circ\text{C}$  for up to 2 h. Samples

were precipitated with ACN, centrifuged at  $2,000 \times g$  for 2 min and analyzed by radio-HPLC.

### Cell Uptake and Receptor Binding Studies

The AR42J rat pancreatic tumor cell line was obtained from ECACC (Salisbury, UK). Cells were cultured in RPMI 1640 medium supplemented with 10% fetal bovine serum and 5 mL of a  $100 \times$  penicillin–streptomycin–glutamine mixture at  $37^\circ\text{C}$  in a humidified 95% air, 5%  $\text{CO}_2$  atmosphere. Media and supplements were purchased from Invitrogen Corporation (Lofer, Austria).

For internalization experiments CCK-2 receptor expressing AR42J cells [22] were seeded at a density of  $1 \times 10^6$  cells per well in six-well plates (Greiner Labortechnik, Kremsmuenster, Austria) and grown to confluency for 48 h. On the day of the experiment, cells were incubated in triplicates with the  $^{111}\text{In}$ -labeled cyclic DOTA-peptides ( $\sim 200$  fmol total peptide) at  $37^\circ\text{C}$  for each time point of 30-min, 1-h and 2-h incubation time. Non-specific binding was determined by a parallel series containing 0.5  $\mu\text{M}$  human minigastrin I (human MG). The cells were treated as described previously [10] and the radioactivity of the collected fractions was counted in a gamma counter. The specifically internalized fraction was expressed in relation to the total activity added (percentage of total activity) as well as in relation to the cell associated activity, *i.e.* internalized plus membrane-bound fraction (percentage of cell bound activity).

### CCK-2 Receptor Autoradiography *In Vitro*

Receptor autoradiography was performed on 20- $\mu\text{m}$ -thick cryostat (Leitz 1720, Rockleigh, NJ) sections of tissue samples of human tumors known from previous studies to express CCK-2 receptors, and with  $^{125}\text{I}$ -D-Tyr-Gly-Asp-Tyr( $\text{SO}_3\text{H}$ )-Nle-Gly-Trp-Nle-Asp-Phe-amide ( $^{125}\text{I}$ -CCK), a radioligand identifying both CCK-1 and CCK-2 receptors, as described elsewhere [23]. The slides were incubated at RT with the radioligand (10,000 cpm/100  $\mu\text{L}$ ) for 150 min. Increasing amounts of DOTA-cyclo-MG1, and of the control peptides DOTA-MG0, DOTA-MG11, and CCK8, were added to generate competitive inhibition curves. Quantification of the autoradiographs obtained using Kodak Biomax MR films (Sigma-Aldrich) and exposure in X-ray cassettes for 7 days was performed using a computer-assisted image-processing system and  $\text{IC}_{50}$  values were calculated. Tissue standards (Amersham, Little Chalfont, UK) were used as reference for quantification. No binding studies were additionally performed with the radiolabeled cyclic DOTA-peptides.

### Evaluation of Biodistribution and Tumor Targeting *In Vivo*

All animal experiments were approved by the institutional animal welfare committees and performed according to national regulations. Biodistribution studies were performed in female athymic BALB/c nude mice (Charles River, Sulzfeld, Germany). For the induction of tumor xenografts, AR42J cells were injected subcutaneously in the right flank at a concentration of  $10 \times 10^6$  in 300  $\mu\text{L}$ .

After 10–15 days, when tumors had reached a size of approximately 0.5 mL, mice were randomly divided into groups of three mice each. Mice were injected intravenously via a lateral tail vein with 0.05 MBq  $^{111}\text{In}$ -DOTA-peptide and 1 MBq  $^{68}\text{Ga}$ -DOTA-peptide simultaneously (corresponding to  $<0.2\ \mu\text{g}$  or  $<0.12\ \text{nmol}$  total peptide). In addition to DOTA-cyclo-MG1 and DOTA-cyclo-MG2, the linear peptide sequence DOTA-linear-MG1 was also studied. Three groups of mice were co-injected with 50  $\mu\text{g}$  human MG to determine whether AR42J uptake was receptor specific. The groups of animals were sacrificed by cervical dislocation 1- or 4-h post-injection (p.i.). Tumors and other tissues (blood, lungs, heart, muscle, spleen, intestines, liver, kidneys, stomach, and pancreas) were removed, weighed, and their radioactivity measured in a gamma counter using appropriate energy windows for  $^{111}\text{In}$  and  $^{68}\text{Ga}$ . Results were expressed as percentage of injected dose per gram tissue (% ID/g). Unpaired *t* test (significance level 0.05) was used for statistical analysis and tumor to organ activity ratios were calculated.

### Small Animal SPECT Imaging Studies

For imaging studies with  $^{111}\text{In}$ -labeled cyclic DOTA-peptide radiolabeling was performed at higher specific activity to reduce the injected peptide amount to a maximum of 0.5  $\mu\text{g}$  peptide (corresponding to 0.3 nmol). The mice were injected with 10–15 MBq  $^{111}\text{In}$ -DOTA-peptide via a tail vein and 1–4-h p.i. imaging was performed under inhaled anesthesia (isoflurane and  $\text{O}_2$ ). Two different mouse xenograft models were available. At the Department of Nuclear Medicine in Nijmegen female BALB/c nude mice ( $n=2$ ) were injected subcutaneously with  $5 \times 10^6$  AR42J rat pancreatic tumor cells in the right flank and tumors were grown for  $<15$  days to reach a size of  $<0.5\ \text{mL}$ . Imaging was performed with a U-SPECT-II/CT animal scanner (MILabs, Utrecht, The Netherlands) using a 1.0-mm-diameter multi-pinhole rat collimator tube (19 bed positions, 60–120 min) and CT images with 60 kV and 45  $\mu\text{A}$  (360 projections, 6 min). Scans were reconstructed with software from MILabs, which uses an ordered-subset expectation maximization algorithm, with a voxel size of 0.375 mm. Images were fused using Inveon Research Workplace software (IRW 3.0, Siemens Precinical Solutions, Knoxville, TN, USA). At the Centre for Molecular Oncology and Imaging, Barts and the London, Queen Mary's School of Medicine and Dentistry in London female beige SCID mice ( $n=2$ ) were injected subcutaneously with  $2 \times 10^6$  A431 epidermoid carcinoma cells transfected with CCK-2 receptor (A431 CCK2-R positive) in the left shoulder and A431 cells transfected with empty vector alone (A431 CCK2-R negative) in the right shoulder and tumors were grown for  $<10$  days to reach a size of  $<0.5\ \text{mL}$ . Imaging was performed using a NanoSPECT/CT four-head camera (Bioscan, Washington DC, USA) fitted with 2-mm pinhole collimators in helical scanning mode (20 projections, 45 min) and CT images with a 45-kVp X-ray source.

## Results

### Radiolabeling

Radiolabeling at elevated temperature of  $95^\circ\text{C}$  resulted in high radiolabeling yields; however for DOTA-cyclo-MG1,

an increasing amount of a side product related to Met oxidation [24] was observed with increased incubation time. To reduce oxidation, radiolabeling at lower temperatures was evaluated. Met(ox) formation was kept below 5% when reacting Met-containing DOTA-cyclo-MG1 at  $80^\circ\text{C}$  for only 5 min with  $^{111}\text{In}$  or  $^{68}\text{Ga}$ . Radiolabeling of Nle-containing DOTA-cyclo-MG2 which is not prone to oxidation was performed at  $90^\circ\text{C}$  with an incubation time of 15 min for  $^{111}\text{In}$  and of 5 min for  $^{68}\text{Ga}$ . Under these conditions, radiochemical purities  $>95\%$  were obtained. Radiolabeling was performed at a specific activity of 2.7–4.1 MBq/nmol peptide with  $^{111}\text{In}$  and of 5.3–13.6 MBq/nmol peptide with  $^{68}\text{Ga}$ . In the radio-HPLC profiles a retention time (tR) in the order of  $^{111}\text{In}$ -DOTA-cyclo-MG1 (6.9 min)  $<$   $^{68}\text{Ga}$ -DOTA-cyclo-MG1 (7.2 min)  $<$   $^{111}\text{In}$ -DOTA-cyclo-MG2 (7.4 min)  $<$   $^{68}\text{Ga}$ -DOTA-cyclo-MG2 (7.7 min) was found.

### Characterization In Vitro and Stability Studies

A summary of the *in vitro* characteristics of  $^{111}\text{In}$ -DOTA-cyclo-MG1 and  $^{111}\text{In}$ -DOTA-cyclo-MG2 is shown in Table 1. Both radioligands showed high stability in aqueous solution with 95.9% to 98.4% intact peptide after 24 h incubation. In human plasma, somewhat lower stability was found for  $^{111}\text{In}$ -DOTA-cyclo-MG1 in comparison with  $^{111}\text{In}$ -DOTA-cyclo-MG2, with 70.0% and 92.3% intact peptide 24 h after incubation, respectively. A higher percentage of metabolites was found for  $^{111}\text{In}$ -DOTA-cyclo-MG1 for all time points studied, whereas oxidation of Met increased only at late time points. Similar protein binding was found for both radioligands, with values of  $20.4 \pm 0.4\%$  for  $^{111}\text{In}$ -DOTA-cyclo-MG1 and  $18.8 \pm 2.0\%$  for  $^{111}\text{In}$ -DOTA-cyclo-MG2 after 4-h incubation. Log *P* values of  $-3.08 \pm 0.12$  for  $^{111}\text{In}$ -DOTA-cyclo-MG1 and  $-2.68 \pm 0.10$  for  $^{111}\text{In}$ -DOTA-cyclo-MG2, and radio-HPLC profiles, indicated a slightly higher lipophilicity for  $^{111}\text{In}$ -DOTA-cyclo-MG2. The metabolic stability studied in rat tissue homogenates revealed complete degradation of both radioligands 2 h after incubation. For both,  $^{111}\text{In}$ -DOTA-cyclo-MG1 and  $^{111}\text{In}$ -DOTA-cyclo-MG2, two main initial metabolites were found, which were further degraded to a final metabolite with low tR.

### Receptor Binding and Internalization

The internalization behavior of both  $^{111}\text{In}$ -DOTA-cyclo-MG1 and  $^{111}\text{In}$ -DOTA-cyclo-MG2 is shown in Fig. 2. For  $^{111}\text{In}$ -DOTA-cyclo-MG1,  $1.74 \pm 0.07\%$  of the total activity added was specifically internalized after 2-h incubation time, whereas for  $^{111}\text{In}$ -DOTA-cyclo-MG2, this value was  $0.93 \pm 0.06\%$  (Fig. 2a). The internalization of the specifically cell-bound activity after 2-h incubation was  $91.3 \pm 0.8\%$  for  $^{111}\text{In}$ -DOTA-cyclo-MG1, whereas for  $^{111}\text{In}$ -DOTA-cyclo-MG2 a somewhat lower value of  $77.8 \pm 1.6\%$  was found (Fig. 2b).



**Table 1.** *In vitro* characteristics of  $^{111}\text{In}$ -DOTA-cyclo-MG1 and  $^{111}\text{In}$ -DOTA-cyclo-MG2

Performed assay	Incubation time	$^{111}\text{In}$ -DOTA-cyclo-MG1	$^{111}\text{In}$ -DOTA-cyclo-MG2
			Percentage of intact peptide (%)
Stability in PBS	4 h	98.7	98.7
	24 h	95.9	98.4
Stability in plasma	4 h	97.0	96.4
	24 h	70.0	92.3
			Percentage of protein binding (%)
Protein binding	1 h	$7.8 \pm 0.5^a$	$13.5 \pm 0.1^a$
	4 h	$20.4 \pm 0.4^a$	$18.8 \pm 2.0^a$
			Log <i>P</i> value
Partition coefficient	15 min	$-3.08 \pm 0.12^a$	$-2.68 \pm 0.10^a$

<sup>a</sup>Protein binding ( $n=2$ ), log *P* ( $n=6$ )

In competition assays on human MTC tissue sections, a very high affinity for the CCK-2 receptor was found for DOTA-cyclo-MG1 with an IC<sub>50</sub> value of  $0.7 \pm 0.12$  nM ( $n=3$ ). A similar value was found also for other CCK-2 analogs analyzed in the same study, with IC<sub>50</sub> values of  $1.0 \pm 0.42$  nM ( $n=3$ ) for DOTA-MG11,  $0.4 \pm 0.12$  nM ( $n=3$ ) for DOTA-MG0, and  $0.06 \pm 0.02$  nM ( $n=3$ ) for the control peptide CCK-8.

### Biodistribution Studies

The biodistribution and tumor targeting of the  $^{111}\text{In}$ - and  $^{68}\text{Ga}$ -labeled DOTA-peptides studied in the AR42J mouse xenograft model at 1- and 4-h p.i. are summarized in Table 2. All radioligands were rapidly cleared from the body mainly through the kidneys. Generally, in most tissues and organs including kidneys, no considerable differences in non-specific tissue retention were observed for

the different  $^{111}\text{In}$ - and  $^{68}\text{Ga}$ -labeled DOTA-peptides. As shown in Fig. 3, the  $^{68}\text{Ga}$ -labeled DOTA-peptides showed higher blood levels when compared to their  $^{111}\text{In}$ -labeled counterparts ( $^{111}\text{In}$ , 0.07–0.39% ID/g;  $^{68}\text{Ga}$ , 0.53–1.21% ID/g) as well as higher uptake in intestines ( $^{111}\text{In}$ , 0.31–0.96% ID/g;  $^{68}\text{Ga}$ , 2.89–6.37% ID/g) and liver ( $^{111}\text{In}$ , 0.21–1.07% ID/g;  $^{68}\text{Ga}$ , 1.85–11.18% ID/g). Interestingly, depending on the radioisotope, tumor uptake varied considerably. For  $^{68}\text{Ga}$ -DOTA-cyclo-MG1 and  $^{68}\text{Ga}$ -DOTA-cyclo-MG2 tumor uptakes of 3.46% and 3.51% ID/g, respectively, were seen at 1-h p.i., whereas  $^{111}\text{In}$ -DOTA-cyclo-MG1 and  $^{111}\text{In}$ -DOTA-cyclo-MG2 only showed 1.10% and 1.20% ID/g tumor uptake, respectively. No significant difference in tumor uptake was observed between  $^{111}\text{In}$  or  $^{68}\text{Ga}$  labeled DOTA-cyclo-MG1 and DOTA-cyclo-MG2 other than a more effective blockage of tumor uptake by co-injection of human MG for DOTA-cyclo-MG1 ( $^{111}\text{In}$ , 50.3%;  $^{68}\text{Ga}$ , 52.2%) in comparison with DOTA-cyclo-MG2 ( $^{111}\text{In}$ , 8.2%;  $^{68}\text{Ga}$ , 42.0%) as well as a more predominant reduction of the tumor retention at the later time

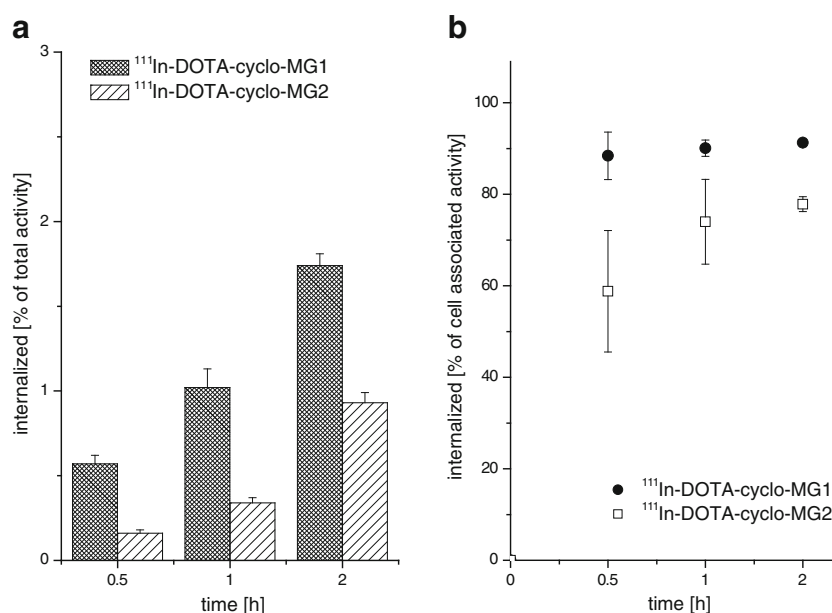


**Fig. 2.** Time-dependent cell-uptake in AR42J cells of  $^{111}\text{In}$ -DOTA-cyclo-MG1 and  $^{111}\text{In}$ -DOTA-cyclo-MG2: (a) internalization expressed as percentage of total activity, (b) internalization expressed as percentage of cell bound activity.

**Table 2.** Biodistribution in AR42J tumor-bearing nude mice of the  $^{111}\text{In}$ - and  $^{68}\text{Ga}$ -labeled DOTA-peptides 1 h and 4 h after injection (tumor uptake 1 h after injection was blocked by co-injection of 50  $\mu\text{g}$  human MG)

Time p.i.	$^{111}\text{In}$ -DOTA-cyclo-MG1			$^{111}\text{In}$ -DOTA-cyclo-MG2			$^{111}\text{In}$ -DOTA-linear-MG1		
	1 h	1 h blocked	4 h	1 h	1 h blocked	4 h	1 h	1 h blocked	4 h
Blood	0.35±0.01	0.20±0.02	0.07±0.06	0.50±0.08	0.39±0.11	0.07±0.01	0.32±0.02	0.13±0.03	0.26±0.02
Lungs	0.54±0.28	0.31±0.08	0.09±0.03	0.58±0.02	1.11±0.79	0.16±0.04	0.32±0.01	0.16±0.02	0.26±0.06
Heart	0.16±0.01	0.11±0.02	0.03±0.03	0.22±0.06	0.18±0.07	0.04±0.01	0.16±0.03	0.08±0.01	0.15±0.01
Muscle	0.08±0.02	0.03±0.01	0.01±0.00	0.23±0.13	0.06±0.02	0.05±0.02	0.08±0.02	0.07±0.04	0.10±0.07
Spleen	0.17±0.03	0.19±0.11	0.12±0.10	0.26±0.03	0.34±0.03	0.22±0.01	0.21±0.03	0.25±0.04	0.15±0.01
Intestines	0.31±0.05	0.28±0.05	0.83±0.77	0.92±0.30	0.96±0.12	0.80±0.44	0.23±0.07	0.35±0.17	0.22±0.03
Liver	0.28±0.06	0.36±0.06	0.21±0.12	0.58±0.09	1.07±0.11	0.39±0.03	0.37±0.03	0.31±0.05	0.30±0.02
Kidneys	2.10±0.47	1.67±0.30	1.84±0.37	2.01±0.20	2.39±0.25	1.43±0.03	2.83±0.20	2.70±0.67	2.71±0.18
Stomach	0.37±0.09	0.20±0.06	0.26±0.11	0.74±0.21	0.27±0.09	0.42±0.11	0.31±0.07	0.11±0.03	0.14±0.05
Pancreas	0.30±0.05	0.23±0.06	0.06±0.03	0.46±0.06	0.64±0.15	0.11±0.02	0.16±0.09	0.06±0.01	0.09±0.02
Tumor	1.10±0.20	0.54±0.10	0.72±0.24	1.20±0.24	1.10±0.06	0.91±0.19	0.37±0.09	0.31±0.04	0.23±0.06
	$^{68}\text{Ga}$ -DOTA-cyclo-MG1			$^{68}\text{Ga}$ -DOTA-cyclo-MG2			$^{68}\text{Ga}$ -DOTA-linear-MG1		
Time p.i.	1 h	1 h blocked	4 h	1 h	1 h blocked	4 h	1 h	1 h blocked	4 h
Blood	1.21±0.04	0.91±0.12	0.53±0.29	1.12±0.25	0.63±0.20	0.65±0.34	0.81±0.01	0.53±0.12	0.87±0.07
Lungs	0.89±0.04	1.22±0.26	0.53±0.10	1.05±0.39	1.38±0.20	0.27±0.12	0.56±0.11	0.43±0.06	0.62±0.23
Heart	0.46±0.06	0.51±0.11	0.26±0.20	0.47±0.20	0.29±0.08	0.15±0.09	0.34±0.00	0.19±0.03	0.36±0.02
Muscle	0.25±0.01	0.23±0.02	0.22±0.10	0.38±0.19	0.09±0.09	0.30±0.08	0.12±0.03	0.09±0.08	0.15±0.06
Spleen	0.73±0.19	0.69±0.05	0.95±0.10	1.62±0.97	2.41±0.23	2.34±0.27	0.33±0.06	0.39±0.09	0.34±0.02
Intestines	3.84±0.15	2.89±0.23	3.19±0.50	5.83±1.50	6.37±0.21	4.82±1.25	0.30±0.06	0.50±0.16	0.32±0.01
Liver	1.85±0.37	2.75±0.09	3.10±0.76	5.59±1.63	11.18±1.83	5.70±0.78	0.52±0.02	0.55±0.09	0.56±0.06
Kidneys	1.48±0.31	1.24±0.20	1.16±0.21	1.57±0.60	1.86±0.29	1.01±0.20	2.26±0.17	2.10±0.52	2.24±0.21
Stomach	1.13±0.21	0.52±0.06	0.96±0.22	1.83±0.19	0.39±0.13	1.06±0.18	0.35±0.10	0.20±0.00	0.28±0.06
Pancreas	0.58±0.26	0.45±0.09	0.31±0.20	0.56±0.17	0.60±0.17	0.27±0.04	0.18±0.03	0.16±0.00	0.19±0.02
Tumor	3.46±0.66	1.66±0.35	2.94±1.00	3.51±1.49	2.04±0.30	3.56±0.64	0.49±0.05	0.65±0.12	0.50±0.04

Values are expressed as percentage of injected dose per gram (mean±SD, n=3)

point. Tumor uptake 4-h p.i. was decreased by 34.2% for  $^{111}\text{In}$ -DOTA-cyclo-MG1 and 15.0% for  $^{68}\text{Ga}$ -DOTA-cyclo-MG1. For  $^{111}\text{In}$ -DOTA-cyclo-MG2, the reduction of tumor uptake 4-h p.i. was 24.0%, while for  $^{68}\text{Ga}$ -DOTA-cyclo-MG2, retained tumor uptake was confirmed. For  $^{111}\text{In}$ - and  $^{68}\text{Ga}$ -DOTA-linear-MG, a very low tumor uptake was observed (0.37% and 0.49% ID/g 1-h p.i., respectively), which was not further reduced by co-injection of human MG. For the receptor expressing organs (stomach and pancreas), generally, a higher uptake was found for  $^{68}\text{Ga}$ -labeled DOTA-peptides in comparison with the  $^{111}\text{In}$ -labeled counterparts. Tumor to organ activity ratios for

blood, muscle, liver, intestines, and kidneys of the  $^{111}\text{In}$ - and  $^{68}\text{Ga}$ -labeled cyclic DOTA-peptides are summarized in Table 3.

### Small Animal SPECT Imaging Studies

For small animal imaging studies a more than 2.5-fold higher peptide amount was injected in comparison with *ex vivo* biodistribution studies in order to perform the imaging with a sufficient amount of radioactivity (10–15 MBq). At the injected dose of 0.3 nmol peptide, a different biodis-

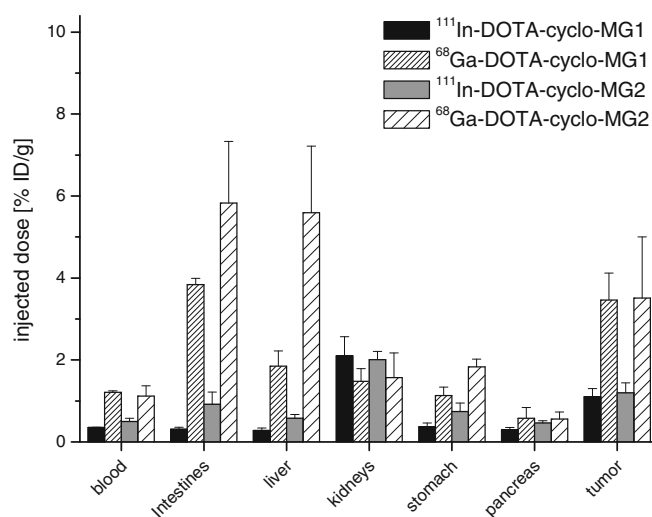


**Fig. 3.** Biodistribution in AR42J tumor-bearing nude mice of the  $^{111}\text{In}$ - and  $^{68}\text{Ga}$ -labeled DOTA-peptides 1 h after injection. Values are expressed as percentage of injected dose per gram (mean±SD, n=3) and are given in Table 2.

**Table 3.** Tissue activity ratios of biodistribution in AR42J tumor-bearing nude mice of  $^{111}\text{In}$ - and  $^{68}\text{Ga}$ -labeled DOTA-cyclo-MG1 and DOTA-cyclo-MG2 1 h after injection

	$^{111}\text{In}$ -DOTA-cyclo-MG1	$^{111}\text{In}$ -DOTA- cyclo-MG2	$^{68}\text{Ga}$ -DOTA- cyclo-MG1	$^{68}\text{Ga}$ -DOTA- cyclo-MG2
Tumor/blood	3.11	2.39	2.47	3.68
Tumor/muscle	10.56	4.19	11.54	12.10
Tumor/liver	3.63	1.99	1.41	0.69
Tumor/intestines	3.23	1.90	0.77	0.71
Tumor/kidneys	0.66	0.60	2.38	2.34

tribution profile was observed. In the AR42J mouse xenograft model (right flank) 1-h p.i., only a faint tumor uptake was observed with  $^{111}\text{In}$ -DOTA-cyclo-MG1 (tumor to kidney activity ratio 0.01), whereas with  $^{111}\text{In}$ -DOTA-cyclo-MG2, the tumor was clearly visible, resulting in a tumor to kidney activity ratio of 0.92 (see Fig. 4). Within a trans-European collaborative project, COST BM0607,  $^{111}\text{In}$ -DOTA-cyclo-MG1 was additionally imaged in beige SCID mice with A431 CCK2-R positive tumors (left shoulder) and A431 CCK2-R negative tumors (right shoulder) using the same peptide amount. In this tumor model, a better tumor uptake could be observed with  $^{111}\text{In}$ -DOTA-cyclo MG1 in the A431 CCK2-R-positive tumor, whereas no uptake was

visible in the A431 CCK2-R-negative tumor. This tumor uptake resulted however in a rather low tumor to kidney activity ratio of 0.35 and 0.28 at 1- and 4-h p.i., respectively (see Fig. 5).

## Discussion

Radiolabeled gastrin and CCK analogs are an emerging new class of radiopharmaceuticals, with promising results in peptide receptor scintigraphy and radionuclide therapy [25, 26]. However, suboptimal pharmacokinetic profiles including unfavorable excretion and rapid metabolism are currently limiting their safe and effective clinical application. In particular, for TRT, the radioactivity delivered to the kidneys has been shown to be the dose-limiting factor.

Radiolabeled MG analogs based on MG0, are characterized by a very high kidney uptake. MG11, without the penta-Glu motif, shows a much lower retention in the

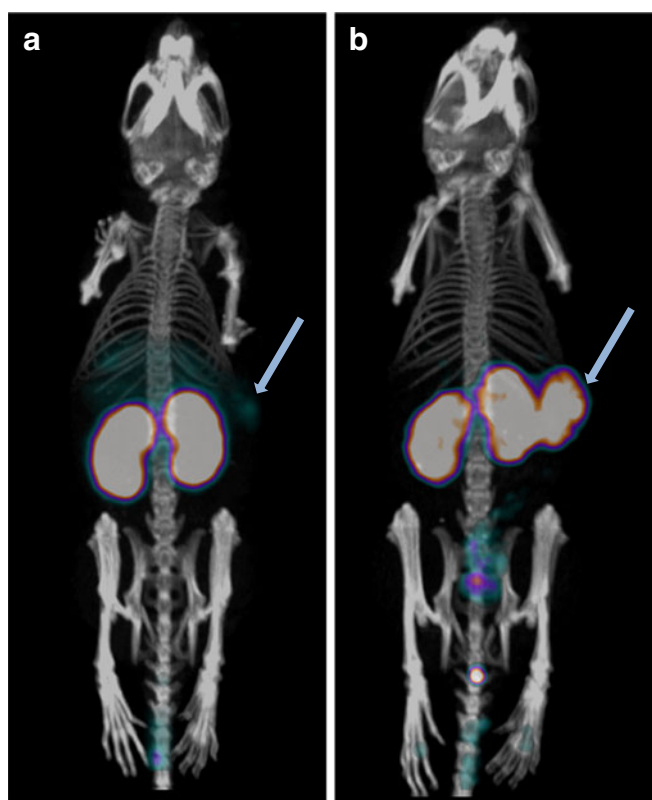


**Fig. 4.** Fused SPECT/CT images of two BALB/c nude mice with AR42J tumor (right flank) 1-h p.i. of  $^{111}\text{In}$ -DOTA-cyclo-MG1 (a) and  $^{111}\text{In}$ -DOTA-cyclo-MG2 (b): Only faint tumor uptake was observed with  $^{111}\text{In}$ -DOTA-cyclo-MG1, whereas with  $^{111}\text{In}$ -DOTA-cyclo-MG2 the tumor was clearly visible (arrows).

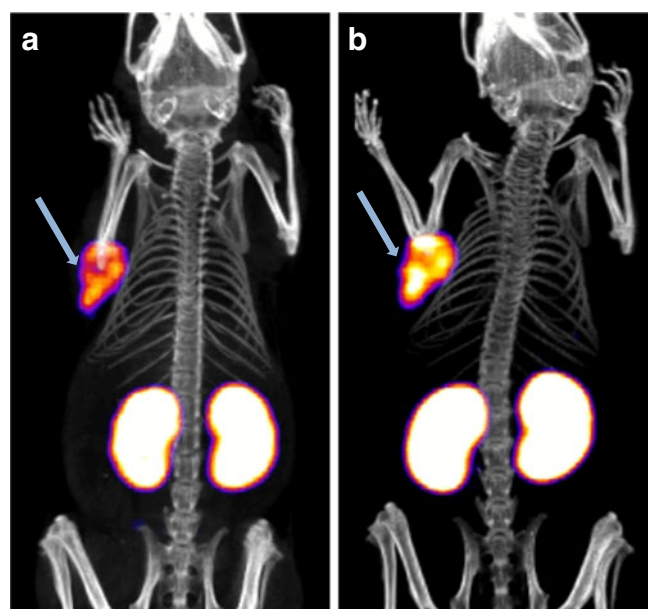


**Fig. 5.** Fused SPECT/CT images of a beige SCID mouse with A431 CCK2-R positive tumor (left shoulder) and A431 CCK2-R negative tumor (right shoulder) 1-h p.i. (a) and 4-h p.i. (b) of  $^{111}\text{In}$ -DOTA-cyclo-MG1: The tumor was clearly visualized in the A431 CCK2-R positive tumor (arrows), whereas no uptake was found in the A431 CCK2-R negative tumor.

kidneys leading to a more than tenfold improvement in the tumor to kidney activity ratio [27]. This change in the peptide structure did, however, considerably reduce the stability of the radioligands *in vivo*. Radioactive metabolites formed *in vivo* can potentially negatively affect the imaging quality and increase the dose to non-target tissue. It therefore seemed necessary to explore alternative stabilization strategies to achieve a combination of high tumor targeting and low side effects. Classical strategies to improve the stability of peptides are D-amino acid substitutions, modification of the N- and C-termini (N-acetylation and C-amidation), replacement of labile amino acids and cyclization. Radiolabeled cyclic SS [28] and RGD [29] analogs display a very high metabolic stability. Based on data available in the literature showing that cyclization of CCK allows the retention of biological activity [30], we decided to study the impact of this modification using MG11 as the lead sequence. Besides cyclization, other approaches to increase the targeting properties of MG analogs could potentially be achieved by dimerization, which has shown to effectively increase tumor uptake while maintaining low kidney retention [31], and possibly also the development of receptor antagonists, a strategy which was successfully applied to SS analogs [32].

Cyclization of MG11 was performed through two modifications in the peptide sequence. D-Glu was incorporated into the peptide sequence through the gamma carboxyl group and Gly was replaced by D-Lys, allowing the introduction of a lactam bridge between the side chain amino group of D-Lys and the  $\alpha$ -carboxyl group of D-Glu. Additionally, the replacement of Met with Nle was studied and the linear peptide sequence was synthesized for comparative studies. Radiolabeling with  $^{111}\text{In}$  and  $^{68}\text{Ga}$  resulted in high radiochemical purity and reasonable specific activity. The optimization of the radiolabeling conditions was especially relevant for Met-containing DOTA-cyclo-MG1. It is known that oxidation of the Met residue in the C-terminal receptor-specific tetrapeptide sequence during the heating step leads to decreased CCK-2 receptor affinity [33, 34] as well as lower cell internalization and tumor uptake [16, 35]. Different radiolabeling strategies have been developed to minimize Met oxidation [33, 36]. We were able to limit Met oxidation to <5% by simply adjusting the reaction conditions in terms of temperature and incubation time. Substitution of Met with Nle resulted in a somewhat higher lipophilicity and protein binding *in vitro* when comparing  $^{111}\text{In}$ -DOTA-cyclo-MG2 with  $^{111}\text{In}$ -DOTA-cyclo-MG1. The  $^{111}\text{In}$ -labeled cyclic DOTA-peptides showed a high stability in solution and plasma, however a higher decline in stability was found for DOTA-cyclo-MG1 at late time points. Stability studies in rat tissue homogenates, looking at proteolytic enzymes present in liver and kidneys [37], revealed a rapid enzymatic degradation of both radioligands. Breeman *et al.* have shown in a pilot clinical study that  $^{111}\text{In}$ -DOTA-MG11 was very rapidly metabolized in blood after injection and this might impair the targeting

efficiency [38]. In a recent study we have evaluated the stability *in vitro* and *in vivo* of a series of gastrin and CCK analogs radiolabeled with  $^{177}\text{Lu}$  including also  $^{177}\text{Lu}$ -DOTA-cyclo-MG1 showing that all conjugates are subjected to a very rapid degradation *in vivo* [39]. To preserve receptor binding, the presence of the intact C-terminal Trp-Met-Asp-Phe-NH<sub>2</sub> sequence seems to be crucial. The possibility to substitute Met with Leu or Nle has already been reported [4], whereas the replacement with other amino acids has been shown to affect receptor affinity [15, 19, 34]. The IC50 value determined for DOTA-cyclo-MG1 in this study compares well with that of DOTA-MG0 and DOTA-MG11, confirming that cyclization does not influence receptor binding. Even though the IC50 value has not been determined also for DOTA-cyclo-MG2, only a minor impairment of receptor binding [19] and reduction of tumor uptake [34] can be expected from this modification. In our previous study with HYNIC-cyclo-MG1 and HYNIC-cyclo-MG2 labeled with  $^{99\text{m}}\text{Tc}$ , we observed a similar dissociation constant for both radiopeptides [21]; therefore, these studies were not performed for the radiolabeled cyclic DOTA-peptides. Cell uptake studies with the radiolabeled cyclic DOTA-peptides showed a somewhat lower internalization compared to that of  $^{111}\text{In}$ -DOTA-MG11 [15]. Substitution of Met with Nle resulted, however, in impaired cell internalization reducing the uptake of the total activity added by >40% and of the cell bound activity by 15% 2 h after incubation.

The biodistribution studies in the AR42J mouse xenograft model revealed some differences between the  $^{111}\text{In}$ - and  $^{68}\text{Ga}$ -labeled cyclic DOTA-peptides.  $^{68}\text{Ga}$ -DOTA-cyclo-MG1 and  $^{68}\text{Ga}$ -DOTA-cyclo-MG2 showed a higher non-specific tissue uptake in most organs (blood, muscle, spleen, intestines, and liver) in comparison with  $^{111}\text{In}$ -DOTA-cyclo-MG1 and  $^{111}\text{In}$ -DOTA-cyclo-MG2. On the other hand, kidney uptake of  $^{68}\text{Ga}$ -labeled cyclic DOTA-peptides was somewhat lower in comparison with the  $^{111}\text{In}$ -labeled counterparts. Even though in cell uptake studies *in vitro* a higher cell uptake was found for  $^{111}\text{In}$ -DOTA-cyclo-MG1 in comparison with  $^{111}\text{In}$ -DOTA-cyclo-MG2, the tumor uptake *in vivo* resulted to be very similar for both peptide analogs. When comparing the  $^{68}\text{Ga}$ - and  $^{111}\text{In}$ -labeled counterparts, tumor uptake was considerably higher for  $^{68}\text{Ga}$ -labeled cyclic DOTA-peptides. This is in contrast with our previous findings with DOTA-MG11 where a comparable tumor uptake was found when labeled with  $^{111}\text{In}$  or  $^{68}\text{Ga}$  [15]. The tumor uptake of the  $^{68}\text{Ga}$ -labeled cyclic DOTA-peptides compares however well with the uptake which we previously found for the cyclic HYNIC-peptides labeled with  $^{99\text{m}}\text{Tc}$  [21]. In comparison with  $^{111}\text{In}$ -DOTA-MG11, a reduction of tumor uptake of >70% was found for  $^{111}\text{In}$ -DOTA-cyclo-MG1 and  $^{111}\text{In}$ -DOTA-cyclo-MG2, whereas for the  $^{68}\text{Ga}$ -labeled counterparts, this reduction was only about 40% [15]. Nevertheless, tumor uptake was shown to be receptor specific as co-injection with human MG resulted in a reduction in uptake of up to 42.0% to 52.2%. Only in



the case of  $^{111}\text{In}$ -DOTA-cyclo-MG2, a minor reduction was found in tumor uptake with human MG (8.2%). No specific tumor uptake was seen for DOTA-linear-MG labeled with  $^{111}\text{In}$  or  $^{68}\text{Ga}$ , confirming that cyclization is required to preserve the receptor binding of these specific MG analogs. A lower flexibility of the cyclic peptide analogs may, however, partly explain the somewhat impaired tumor targeting *in vivo*. The finding of a higher tumor uptake of  $^{68}\text{Ga}$ -labeled cyclic DOTA-peptides could potentially be related to a higher receptor affinity. Also for SS analogs, a better receptor affinity profile was found for labeling with  $^{68}\text{Ga}$  in comparison with  $^{111}\text{In}$  [40, 41] leading to improved tumor detection in humans [42]. Additionally, a different complex geometry was reported for  $^{111}\text{In}$  and  $^{68}\text{Ga}$  influencing the pharmacological properties of the radiopeptides [43]. In a previous study, we found, however, a very similar tumor uptake and biodistribution profile for  $^{111}\text{In}$ - and  $^{68}\text{Ga}$ -labeled DOTA-MG11 [15]. Tumor uptake 4-h p.i. with values of 0.72% and 0.91% ID/g for  $^{111}\text{In}$ -labeled and 2.94% and 3.56% ID/g for  $^{68}\text{Ga}$ -labeled DOTA-cyclo-MG1 and DOTA-cyclo-MG2 compares well with other MG analogs studied in the same tumor model [34]. Target to non-target activity ratios calculated from the *ex vivo* biodistribution were shown to be highest for  $^{68}\text{Ga}$ -DOTA-cyclo-MG2 for blood, muscle, and kidneys, but due to the higher uptake of  $^{68}\text{Ga}$ -labeled cyclic DOTA-peptides in intestines and liver, the balance tips in favor of  $^{111}\text{In}$ -DOTA-cyclo-MG1. In the imaging studies performed with both  $^{111}\text{In}$ -labeled cyclic DOTA-peptides in the same mouse xenograft model,  $^{111}\text{In}$ -DOTA-cyclo-MG2 was, however, clearly superior in visualizing the tumor. This may possibly be explained by the higher peptide amount injected which was required to achieve high-contrast images. A possible influence of the injected peptide mass on the biodistribution behavior was reported also for SS analogs [44]. Tumor uptake of radiolabeled DOTA-cyclo-MG2 also shows a higher retention over time. Therefore, the difference in tumor uptake could possibly also be related to the somewhat higher stability and lipophilicity observed with this peptide analog. Besides differences in receptor density, tumor growth rate, and vascularization, the biology of the tumor may also have a significant influence on the tumor uptake. In the AR42J mouse xenograft model based on rat pancreatic tumor cells,  $^{111}\text{In}$ -DOTA-cyclo-MG1 almost failed to detect the tumor, whereas with the A431 CCK2-R-positive model based on an epidermoid carcinoma cell line transfected with the human CCK-2 receptor, a higher uptake was observed.

## Conclusion

Two novel MG11-based cyclic peptide analogs derivatized with DOTA for radiolabeling with trivalent radiometals have been developed. Receptor binding *in vitro* was preserved after cyclization, and even though some drawbacks regarding cell internalization and receptor targeting in the mouse xenograft model were observed for the radiolabeled peptide

analog, their tumor uptake *in vivo* compares well with that of other radiolabeled MG analogs developed. Cyclization resulted in a higher stability of the radioligands in plasma, however did not considerably improve the metabolic stability in tissue homogenates. In further studies, we will try to elucidate if an improvement in metabolic stability is necessary to increase the targeting properties and the pharmacokinetic profile of MG analogs. These studies will base on the characterization of the metabolites formed during degradation to develop new stabilization strategies. Still, the described cyclic MG analogs seem to be promising for clinical application in CCK-2 targeting and contribute to the development of safe and efficient MG-based radiopharmaceuticals for imaging and therapy of MTC and other CCK-2 expressing tumors.

**Acknowledgments.** We would like to thank Werner Sallegger from piCHEM Research and Development (Graz, Austria) for synthesizing the peptide derivatives used in this study. Lieke Joosten (Radboud University Nijmegen Medical Centre) is acknowledged for expert help in radiolabeling. Ciara Finucane, Jerome Burnet, and Julie Foster assisted in the imaging studies carried out at Barts and the London, Queen Mary's School of Medicine and Dentistry. Collaboration within the COST Action BM0607 "Targeted Radionuclide Therapy (TRNT)" is greatly acknowledged. This work was supported by grants from the Austrian Nano Initiative (Nano-Health consortium, Project N208-NAN) and was partly performed within the PhD program Image Guided Diagnosis and Therapy (IGDT) of the Medical University Innsbruck, Austria.

**Conflict of interest.** The authors declare that they have no conflict of interest.

## References

1. Kwekkeboom DJ, de Herder WW, van Eijck CH, Kam BL, van Essen M, Teunissen JJ, Krenning EP (2010) Peptide receptor radionuclide therapy in patients with gastroenteropancreatic neuroendocrine tumors. *Semin Nucl Med* 40:78–88
2. Virgolini JJ, Gabriel M, von Guggenberg E, Putzer D, Kendler D, Decristoforo C (2009) Role of radiopharmaceuticals in the diagnosis and treatment of neuroendocrine tumours. *Eur J Cancer* 45:S274–S291
3. Reubi JC (2007) Targeting CCK receptors in human cancers. *Curr Top Med Chem* 7:1239–1242
4. Behe M, Behr TM (2002) Cholecystokinin-B (CCK-B)/gastrin receptor targeting peptides for staging and therapy of medullary thyroid cancer and other CCK-B receptor expressing malignancies. *Biopolymers* 66:399–418
5. Behr TM, Gotthardt M, Barth A, Behe M (2001) Imaging tumors with peptide-based radioligands. *Q J Nucl Med* 45:189–200
6. Gotthardt M, Béhé MP, Beuter D, Battmann A, Bauhofer A, Schurrat T, Schipper M, Pollum H, Oyen WJ, Behr TM (2006) Improved tumour detection by gastrin receptor scintigraphy in patients with metastasised medullary thyroid carcinoma. *Eur J Nucl Med Mol Imaging* 33:1273–1279
7. Gotthardt M, Béhé MP, Grass J, Bauhofer A, Rinke A, Schipper ML, Kalinowski M, Arnold R, Oyen WJ, Behr TM (2006) Added value of gastrin receptor scintigraphy in comparison to somatostatin receptor scintigraphy in patients with carcinoids and other neuroendocrine tumours. *Endocr Relat Cancer* 13:1203–1211
8. Laverman P, Roosenburg S, Gotthardt M, Park J, Oyen WJ, de Jong M, Hellmich MR, Rutjes FP, van Delft FL, Boerman OC (2008) Targeting of a CCK<sub>2</sub> receptor splice variant with  $^{111}\text{In}$ -labelled cholecystokinin-8 (CCK8) and  $^{111}\text{In}$ -labelled minigastrin. *Eur J Nucl Med Mol Imaging* 35:386–392
9. Béhé M, Becker W, Gotthardt M, Angerstein C, Behr TM (2003) Improved kinetic stability of DTPA- dGlu as compared with conventional monofunctional DTPA in chelating indium and yttrium: preclinical and initial clinical evaluation of radiometal labelled minigastrin derivatives. *Eur J Nucl Med Mol Imaging* 30:1140–1146

10. von Guggenberg E, Behe M, Behr TM, Saurer M, Seppi T, Decristoforo C (2004)  $^{99m}\text{Tc}$ -Labeling, *in vitro* and *in vivo* evaluation of HYNIC and (Na-His)-acetic acid modified [D-Glu1]-Minigastrin. *Bioconjug Chem* 15:864–871
11. Nock BA, Maina T, Behe M, Nikolopoulou A, Gotthardt M, Schmitt JS, Behr TM, Macke HR (2005) CCK-2/gastrin receptor-targeted tumor imaging with  $^{99m}\text{Tc}$ -labeled minigastrin analogs. *J Nucl Med* 46:1727–1736
12. Melis M, Krenning EP, Bernard BF, de Visser M, Rolleman E, de Jong M (2007) Renal uptake and retention of radiolabeled somatostatin; bombesin; neurotensin; minigastrin and CCK analogs: species and gender differences. *Nucl Med Biol* 34:633–641
13. Béhé M, Kluge G, Becker W, Gotthardt M, Behr TM (2005) Use of polyglutamic acids to reduce uptake of radiometal-labeled minigastrin in the kidneys. *J Nucl Med* 46:1012–1015
14. Behe M, Reubi J, Nock B, Mäcke H, Breeman WAP, Bernard HF, Behr TM, De Jong M (2005) Evaluation of a DOTA-minigastrin derivative for therapy and diagnosis for CCK-2 receptor positive tumours. *Eur J Nucl Med Mol Imaging* 32:S78
15. Helbok A, Decristoforo C, Behe M, Rangger C, von Guggenberg E (2009) Preclinical evaluation of In-111 and Ga-68 labelled minigastrin analogues for CCK-2 receptor imaging. *Current Radiopharm* 2:304–310
16. von Guggenberg E, Dietrich H, Skvortsova I, Gabriel M, Virgolini IJ, Decristoforo C (2007)  $^{99m}\text{Tc}$ -labelled HYNIC-minigastrin with reduced kidney uptake for targeting of CCK-2 receptor-positive tumours. *Eur J Nucl Med Mol Imaging* 34:1209–1218
17. Nikolopoulou A, Nock BA, Petrou C, Ketani E, Cordopatis P, Maina T (2006) *In vivo* targeting of CCK-2/Gastrin-R and reduction of renal accumulation with truncated  $^{99m}\text{Tc}$ Demogastrin 4–6. In: Mazzi U, Giron MC, Nadali A, Rossin R (eds) *Technetium, Rhenium and Other Materials in Chemistry and Nuclear Medicine 7*. SGEEditoriali, Padova, pp 325–326
18. Kosowicz J, Mikołajczak R, Czepczyński R, Ziemnicka K, Gryczyńska M, Sowiński J (2007) Two peptide receptor ligands  $^{99m}\text{Tc}$ -EDDA/HYNIC-Tyr<sub>3</sub>-octreotide and  $^{99m}\text{Tc}$ -EDDA/HYNIC-DGlu<sub>1</sub>-octagastrin for scintigraphy of medullary thyroid carcinoma. *Cancer Biother Radiopharm* 22:613–628
19. Good S, Walter MA, Waser B, Wang X, Müller-Brand J, Béhé MP, Reubi JC, Maecke HR (2008) Macrocyclic chelator-coupled gastrin-based radiopharmaceuticals for targeting of gastrin receptor-expressing tumours. *Eur J Nucl Med Mol Imaging* 35:1868–1877
20. Stone SR, Giragossian C, Mierke DF, Jackson GE (2007) Further evidence for a C-terminal structural motif in CCK2 receptor active peptide hormones. *Peptides* 28:2211–2222
21. von Guggenberg E, Sallegger W, Helbok A, Ocak M, King R, Mather SJ, Decristoforo C (2009) Cyclic Minigastrin analogues for gastrin receptor scintigraphy with Technitium-99 m: preclinical evaluation. *J Med Chem* 52:4786–4793
22. Svoboda M, Dupuche MH, Lambert M, Bui D, Christophe J (1990) Internalization-sequestration and degradation of cholecystokinin (CCK) in tumoral rat pancreatic AR 4–2 J cells. *Biochim Biophys Acta* 1055:207–216
23. Reubi JC, Schaefer JC, Waser B (1997) Cholecystokinin(CCK)-A and CCK-B/gastrin receptors in human tumors. *Cancer Res* 57:1377–1386
24. Ocak M, Decristoforo C, Rangger C, Helbok A, Sallegger W, von Guggenberg E (2009)  $^{177}\text{Lu}$ -DOTA-cyclogastrin: stability assessment and evaluation *in vitro*. *J Label Compd Radiopharm* 52:S514
25. de Visser M, Verwijnen SM, de Jong M (2008) Update: improvement strategies for peptide receptor scintigraphy and radionuclide therapy. *Cancer Biother Radiopharm* 23:137–157
26. Reubi JC, Maecke HR (2008) Peptide-based probes for cancer imaging. *J Nucl Med* 49:1735–1738
27. Trejtnar F, Laznickova M, Laznickova A, Kopecky M, Petrik M, Béhé M, Schmidt J, Maecke H, Maina T, Nock B (2007) Biodistribution and elimination characteristics of two  $^{111}\text{In}$ -labeled CCK-2/gastrin receptor-specific peptides in rats. *Anticancer Res* 27:907–912
28. Cremonesi M, Ferrari M, Zoboli S, Chinol M, Stabin MG, Orsi F, Maecke HR, Jermann E, Robertson C, Fiorenza M, Tosi G, Paganelli G (1999) Biokinetics and dosimetry in patients administered with  $^{111}\text{In}$ -DOTA-Tyr(3)-octreotide: implications for internal radiotherapy with  $^{90}\text{Y}$ -DOTATOC. *Eur J Nucl Med* 26:877–886
29. Decristoforo C, Hernandez Gonzalez I, Carlsen J, Rupprich M, Huisman M, Virgolini I, Wester HJ, Haubner R (2008)  $^{68}\text{Ga}$ - and  $^{111}\text{In}$ -labelled DOTA-RGD peptides for imaging of alphavbeta3 integrin expression. *Eur J Nucl Med Mol Imaging* 35:1507–1515
30. Charpentier B, Pelaprat D, Durieux C, Dor A, Reibaud M, Blanchard JC, Roques BP (1988) Cyclic cholecystokinin analogs with high selectivity for central receptors. *Proc Natl Acad Sci USA* 85:1968–1972
31. Sosabowski J, Matzow T, Foster J, Mather S (2008) Targeting of CCK2 receptor expressing tumours using an  $^{111}\text{In}$ -labelled minigastrin dimer. *Q J Nucl Med Mol Imaging* 52:S13
32. Akgün E, Körner M, Gao F, Harikumar KG, Waser B, Reubi JC, Portoghese PS, Müller LJ (2009) Synthesis and *in vitro* characterization of radioiodinatable benzodiazepines selective for type 1 and type 2 cholecystokinin receptors. *J Med Chem* 52:2138–2147
33. Breeman WAP, de Blois E, van Gameren A, Melis M, Fröberg A, de Jong M, Mäcke H, Krenning EP (2006) Aspects of CCK-2 receptor-targeting with  $^{111}\text{In}$ -DOTA-MG. In: Mazzi U, Giron MC, Nadali A, Rossin R (eds) *Technetium, rhenium and other materials in Chemistry and Nuclear Medicine 7*. SGEEditoriali, Padova, pp 231–232
34. Mather SJ, McKenzie AJ, Sosabowski JK, Morris TM, Ellison D, Watson SA (2007) Selection of radiolabeled gastrin analogs for peptide receptor-targeted radionuclide therapy. *J Nucl Med* 48:615–622
35. Maina T, Nikolopoulou A, Ketani E, Petrou C, Cordopatis P, Nock BA (2006) Oxidation—Nle<sup>11</sup>/Mox<sup>11</sup> replacement of Met<sup>11</sup> in  $^{99m}\text{Tc}$  demogastrin 2: effects on CCK-2/gastrin-R-interaction. In: Mazzi U, Giron MC, Nadali A, Rossin R (eds) *Technetium, rhenium and other materials in Chemistry and Nuclear Medicine 7*. SGEEditoriali, Padova, pp 323–324
36. Sosabowski JK, Lee M, Dekker BA, Simmons BP, Singh S, Beresford H, Hagan SA, McKenzie AJ, Mather SJ, Watson SA (2007) Formulation development and manufacturing of a gastrin/CCK-2 receptor targeting peptide as an intermediate drug product for a clinical imaging study. *Eur J Pharm Sci* 31:102–111
37. Werle M, Bernkop-Schnürch A (2006) Strategies to improve plasma half life time of peptide and protein drugs. *Amino Acids* 30:351–367
38. Breeman WA, Froberg AC, de Blois E, van Gameren A, Melis M, de Jong M, Maina T, Nock BA, Erion JL, Maecke HR, Krenning EP (2008) Optimised labeling, preclinical and initial clinical aspects of CCK-2 receptor-targeting with 3 radiolabeled peptides. *Nucl Med Biol* 35:839–849
39. Ocak M, Helbok A, Rangger C, Peitl PK, Nock BA, Morelli G, Eek A, Sosabowski JK, Breeman WA, Reubi JC, Decristoforo C (2011) Comparison of biological stability and metabolism of CCK2 receptor targeting peptides, a collaborative project under COST BM0607. *Eur J Nucl Med Mol Imaging* (in press)
40. Reubi JC, Schär JC, Waser B, Wenger S, Heppeler A, Schmitt JS, Mäcke HR (2000) Affinity profiles for human somatostatin receptor subtypes SST1–SST5 of somatostatin radiotracers selected for scintigraphic and radiotherapeutic use. *Eur J Nucl Med* 27:273–282
41. Ginj M, Chen J, Walter MA, Eltschinger V, Reubi JC, Maecke HR (2005) Preclinical evaluation of new and highly potent analogues of octreotide for predictive imaging and targeted radiotherapy. *Clin Cancer Res* 11:1136–1145
42. Gabriel M, Decristoforo C, Kendler D, Dobrozemsky G, Heute D, Uprimny C, Kovacs P, von Guggenberg E, Bale R, Virgolini IJ (2007)  $^{68}\text{Ga}$ -DOTA-Tyr3-octreotide PET in neuroendocrine tumors: comparison with somatostatin receptor scintigraphy and CT. *J Nucl Med* 48:508–518
43. Antunes P, Ginj M, Zhang H, Waser B, Baum RP, Reubi JC, Maecke H (2007) Are radiogallium-labelled DOTA-conjugated somatostatin analogues superior to those labelled with other radiometals? *Eur J Nucl Med Mol Imaging* 34:982–993
44. de Jong M, Breeman WA, Bernard BF, van Gameren A, de Bruin E, Bakker WH, van der Pluijm ME, Visser TJ, Mäcke HR, Krenning EP (1999) Tumour uptake of the radiolabelled somatostatin analogue [DOTA0, Tyr3]octreotide is dependent on the peptide amount. *Eur J Nucl Med* 26:693–698